BOLD response to spatial phase congruency in human brain

Andrea Perna Scuola Normale Superiore, Istituto di Neuroscienze CNR, Pisa, Italy

Michela Tosetti Istituto Scientifico Stella Maris, Pisa, Italy

Domenico Montanaro Istituto di Fisiologia Clinica CNR-CREAS, Pisa, Italy

Maria Concetta Morrone Istituto Scientifico Stella Maris, Pisa, Italy, & Facoltà di Medicina, Università degli Studi di Pisa, Pisa, Italy

Human psychophysical observations, computational models, and the selectivity of neurons in primary visual cortex all suggest that an early step in visual processing is the detection of features such as lines and edges. However, previous fMRI experiments investigating the responses of early visual areas to phase coherence have led to apparently discordant results. We studied the human brain BOLD responses to structured periodic band-pass images of matched amplitude spectrum but of different phase spectra, arranged to create three distinct types of stimuli: pure edges; pure lines (matched global and local energy to the edges, but different phase); and random noise (random phase spectrum, hence no salient features, and a different spatial distribution of local energy from the lines and edges stimuli). Alternation of lines against edges did not activate primary visual cortex, but did activate two higher order visual areas. Alternation of these lines or edges against the random stimulus produced a strong activity in many visual areas, including primary visual cortex. Interestingly, the BOLD activity was higher for the edges and lines than for the random stimuli for a wide range of stimulus contrasts, indicating the presence of non-linear gain modulation in the cell response. These results show that phase congruency is coded at the level of primary visual cortex. We show that a stage of response gain modulation can explain our present and previous fMRI discordant results.

Keywords: visual cortex, spatial vision, functional imaging, contrast gain, receptive fields, shape and contour

Citation: Perna, A., Tosetti, M., Montanaro, D., & Morrone, M. C. (2008). BOLD response to spatial phase congruency in human brain. *Journal of Vision, 8*(10):15, 1–15, http://journalofvision.org/8/10/15/, doi:10.1167/8.10.15.

Introduction

Phase information dominates perception of visual scenes: phase spectra, rather than amplitude spectra determine the appearance of the images (Morgan, Ross, & Hayes, 1991; Openheim & Lim, 1981; Piotrowski & Campbell, 1982; Shapley, Caelli, Grossberg, Morgan, & Rentschler, 1990; Tadmor & Tolhurst, 1993; Wichmann, Braun, & Gegenfurtner, 2006). Humans are highly sensitive to phase and can discriminate small variations (about 10 deg) particularly around line and edge phase alignment (Burr, 1980; Burr, Morrone, & Spinelli, 1989; Field & Nachmias, 1984; Martini, Girard, Morrone, & Burr, 1996; Morrone, Burr, & Spinelli, 1989). The specificity for phase is thought to be associated with neuronal circuits in early visual processing devoted to an efficient representation of relevant image attributes, such as object boundaries (usually associated with line and edge luminance profiles). Efficient representation is achieved when the structure of the receptive field matches the essential profile of the target feature (matched filter), conferring to the neuron a high sensitivity and selectivity for that particular class of features. Thus, odd-symmetric receptive fields would preferably code edges, while even-symmetric receptive fields line-like luminance profiles.

Many primary visual cortical neurons have a quasi-linear response (e.g., Hubel & Wiesel, 1962; Movshon, Thompson, & Tolhurst, 1978a, 1978b, for review see Ringach, 2004), and their receptive fields are well described by Gabor wavelet functions of different sizes, orientations, and phase. Neurons of cat area 17 show a uniform distribution for preference of spatial phases (Field & Tolhurst, 1986; Gaska, Pollen, & Cavanagh, 1987; Jones & Palmer, 1987; Pollen, Gaska, & Jacobson, 1988) and current theories of independent component analysis or sparse coding demonstrate that this is an efficient strategy for feature analysis (Hyvärinen & Hoyer, 2001; Olshausen & Field, 1996; van Hateren & Ruderman, 1998). However a more recent experiment on monkey primary visual cortex (Ringach, 2002) found a bimodal distribution of spatial phase encoding, with neuronal receptive fields clustering into even- and odd-symmetric classes.

doi: 10.1167/8.10.15 Received December 13, 2007; published December 22, 2008 ISSN 1534-7362

The analysis of the perceptual structure of multi-harmonic patterns suggested an alternative mechanism for the high performance in phase discrimination and the peculiar sensitivity to phase spectra: the brain may not code directly phase *per se* but may perform an analysis of congruency between the various harmonic component phases (Morrone & Owens, 1987; Morrone, Ross, Burr, & Owens, 1986; Ross, Morrone, & Burr, 1989). Salient spatial points in the luminance distribution have been demonstrated to correspond to points where the various harmonics have the same phase alignment (phase congruency). The *local energy* model of feature detection (Burr & Morrone, 1992; Morrone & Burr, 1988; Morrone & Owens, 1987) is based on this idea and has proven successful in predicting perceptual appearance and in segmenting visual scenes (real and illusory) on the basis of position of the detected features (Kovesi, 1999; Morrone & Burr, 1997; Morrone, Burr, & Ross, 1994; Perna & Morrone, 2007). The model comprises a first stage that computes a local energy function from the sum of the squared responses of visual operators with even and odd symmetry receptive fields: peaks in this (local energy) function correspond to salient features. The second stage classifies the type of feature by evaluating the relative response of operators with odd and even receptive fields (corresponding to an evaluation of phase at sparse positions).

The squaring operation is thought to correspond to the activity of complex cells, whose receptive field is usually modeled as the quadrature pair summation of two subunits with Gabor receptive fields at sine and cosine phases, respectively (Adelson & Bergen, 1985; Emerson, Korenberg, & Citron, 1992; Gaska, Jacobson, Chen, & Pollen, 1994; Pollen et al., 1988; Shams & von der Malsburg, 2002; Spitzer & Hochstein, 1985a, 1985b; Szulborski & Palmer, 1990; Touryan, Felsen, & Dan, 2005). The Gabor subunits resemble striate simple cells, except for the absence of half-wave rectification. Each Gabor subunit can be viewed, therefore, as representing the pooled output of a pair of simple cells with opposite contrast polarities. The advantage of the quadratic operation between subunits is to confer to the neuron a high selectivity to spectral phase congruency (Morrone & Burr, 1988; Morrone & Owens, 1987) and hence an efficient strategy to locate important features without necessarily being selective to a particular feature class (edge versus lines).

Only a few studies have investigated directly the selectivity of single neurons to phase congruency. Felsen, Touryan, Han, and Dan (2005, Touryan et al., 2005) reported a stronger response of complex cells of cat area 17 to natural images versus the noisy pattern obtained by scrambling the phase spectra. Mechler, Ohiorhenuan, and Victor (2007) and Mechler, Reich, and Victor (2002) have shown that both simple and complex cells are sensitive to the value of the alignment phases of harmonic components, with some cells strongly tuned for phase and practically no cell invariant to the phase transformation. While these effects are not accounted for by the simple two-stage energy model as proposed by Burr and Morrone (1992) and Morrone and Burr (1988), they indicate that phase sensitivity is already coded at the level of cat area 17.

Many fMRI studies in human and monkeys compared the response to natural images to those derived by scrambling the location of the image pixels (Epstein & Kanwisher, 1998; Grill-Spector et al., 1998; Kanwisher, McDermott, & Chun, 1997; Kourtzi & Kanwisher, 2000; Rainer, Augath, Trinath, & Logothetis, 2002). The results showed that a preference for natural images is established only later in the visual analysis with primary visual cortex preferring slightly the scrambled images. However, the increase of the response for random images may reflect the increased high spatial frequency content of scrambled images. Only a few recent studies investigated the brain responses to complex stimuli manipulating directly the phase spectrum and these gave somewhat different results.

Olman, Ugurbil, Schrater, and Kersten (2004) measured the BOLD contrast responses in human early visual areas for natural and whitened images and for pink and white noise images, presented in rapid succession against an equiluminant background. They found no significant effect of increased spatial phase coherence in natural images on the BOLD response of V1. They suggest that V1 activity correlates better with the contrast of the images than with the phase spectrum. Tjan, Lestou, and Kourtzi (2006) also measured the response of natural images contaminated by noise of matched power spectra. The data showed an increase of the BOLD response as a function of phase congruency in V1 only in half of the subjects tested. The preference for the natural image increased gradually both along the ventral and the dorsal pathways. These data contrast with those of Rainer, Augath, Trinath, and Logothetis (2001) on the macaque primary visual cortex that show a clear preference for natural images with respect to random phase pattern. Unfortunately, the dependence of the response as function of coherence cannot be assessed from these data due to an artefact in the stimulus presentation (see Dakin, Hess, Ledgeway, & Achtman, 2002).

Here we use an fMRI paradigm to measure the phase responses in human visual brain. At different levels of stimulus contrast, we compared the BOLD responses to visual stimuli comprising edges (Figure 1A), lines (Figure 1B), or noise with the same power spectrum of the edge and line stimuli but with random phase (Figure 1C). Different patterns of neuronal responses are expected if the activity in a brain area is mainly driven by stimulus contrast (Michelson or Root Mean Square contrast—RMS), or by phase value and phase coherence among spatial harmonics that compose the stimulus. Unlike previous studies, we use patterns with band-pass amplitude spectra that should optimize the selectivity to phase congruency if it exists. The results indicate selectivity to phase congruency as early as in V1 but an

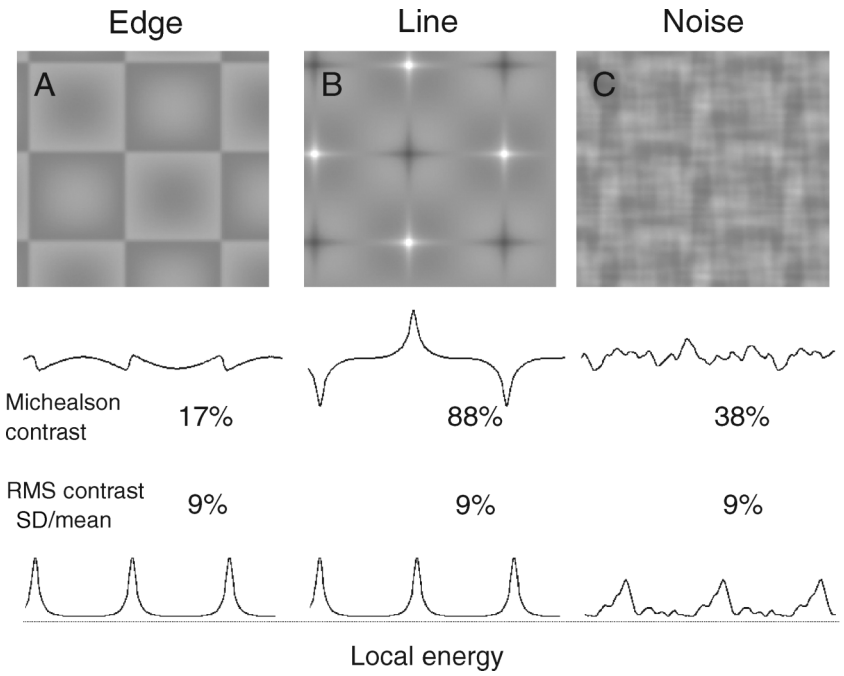

Figure 1. Examples of the visual stimuli. (A) The stimuli used in the experiment were high pass filtered checkerboards (missing fundamental), comprising four cycles along the horizontal axis and three cycles along the vertical axis. Each cycle of the checkerboard—one dark and one light square—was 7.5 deg of visual angle wide. (B) The Hilbert transform of the stimulus in (A), where edges have been transformed into lines. (C) Noise stimulus obtained by scrambling the phase of the checkerboard stimulus in (A). All the stimuli have the same RMS contrast but very different Michelson contrasts. Stimuli in (A) and (B), but not in (C), have the same local energy distribution.

invariance of the response to the particular phase value (line or edge). The invariance seems to be resolved only later in the Lateral Occipital and Intraparietal cortices.

Methods

Visual stimuli

The three different stimuli used in the experiment are shown in Figure 1.

The "Edge" stimulus (Figure 1A) is a two-dimensional missing-fundamental checkerboard, comprising 8 × 6 squares each subtending 3.75 × 3.75 degrees of visual angle. The fundamental harmonics were removed to prevent BOLD signals from being determined by these higher amplitude harmonics, irrespective of phase congruency. In addition, the high and low spatial frequencies were attenuated with a Gaussian filter given by

$$G(\omega) = \exp\left(-\omega^2/2\sigma_K^2\right) - \exp\left(-\omega^2/2\sigma_L^2\right), \qquad (1)$$

where ω is the spatial frequency and σ_K = 4.27 and σ_L = 0.17 c/deg.

The "Line" stimulus (Figure 1B) was designed to have, both locally and globally, an amplitude spectrum identical to that of the edge stimulus, but a different phase spectrum, with edges replaced by lines. This was achieved by applying a Hilbert transform to the original function: the phase spectrum of each row of the original image was increased by $\pi/2$, multiplied by the sign function, then transformed in space by inverse Fourier transform. The same procedure was then applied for each column (see Morrone & Burr, 1997 for further details of methods). These two stimuli will be referred to as "coherent phase stimuli."

The random noise stimuli (Figure 1C) had exactly the same amplitude spectrum as the edge and line stimuli and the same spatial periodicity, but the phase of each component was shifted by a random value. Hence, while all the stimuli have the same RMS contrast and amplitude spectra, the phase coherence and local energy distribution is very different for the noise stimuli. Examples of the luminance profiles, the Michelson contrast, the RMS contrast, and the local energy of the three stimuli are reported in Figure 1. The luminance profiles are very different for the three stimuli, producing Michelson contrasts five times higher for the line stimulus than for the edge stimulus. The noise stimuli have on average intermediate Michelson contrasts.

Stimuli were generated in advance as AVI uncompressed movies in MATLAB (245 gray levels) and displayed at 60 Hz through liquid crystal goggles (VisuaStim XGA—Resonance Technology at a resolution of 800 × 600 pixels, subtending 30° × 22.5° at an apparent distance of 1.2 m, with mean luminance of about 30 cd/m^2 and equipped with an infrared 60-Hz telecamera for monitoring eye movements). Extreme care was taken to gamma-correct and linearize the system. We first measured the luminance of a full field linear increment displayed on the same goggles, driven by the same PC and generated with the same MATLAB program, using a Minolta photometer (Chromameter) attached to the liquid crystal. We then used the fitted luminance gray-level functions to linearize the luminance profile of the stimuli. As an additional check we matched psychophysically the apparent luminance of each luminance step displayed on the goggles with the apparent luminance of an additional monitor whose luminance could easily be calibrated by the photometer. The AVI movie comprised an alternation of three "OFF" epochs and three "ON" epochs, each presented for 30 s. The first epoch was 12 s longer to achieve BOLD signal stabilization.

A block design was used for all experiments, where the coherent and noise stimuli were contrasted in different combinations, as illustrated in Figure 2. In a first condition (schematically illustrated in Figure 2, left), edge (Figure 1A) and line (Figure 1B) stimuli were contrasted with each other. In the "ON" epoch the edge stimulus was displayed, at 15 different spatial positions, updated every 2 s. During the "OFF" epoch, the line stimuli were displayed, again in 15 random positions, updated every 2 s (the refresh procedure was adopted to prevent BOLD signal adaptation). In this condition the ON and OFF epoch stimuli have different values of Michelson contrast and are perceptually quite different, although they have the same phase coherence between harmonics and the same local energy. In the second condition (schematically illustrated in Figure 2, right), the ON epoch comprised both edge and line stimuli, randomly chosen (with equal probabilities) and presented at random position every 2 s. These coherent stimuli were contrasted with the noise stimulus presented in the OFF epoch (again, shifting both stimuli to random positions every 2 s). In this condition, the stimuli presented in the ON and OFF epochs have on average the same Michelson and RMS contrast, as well as the same total energy, but the stimuli in the ON epoch always have higher phase coherence.

For all conditions, the fixation target remained stable in the center of the visible screen of the goggles, and the stimuli extended over the full visible 30° × 22.5° of visual field, comprising 8 × 6 periods.

The experiment contrasting coherent stimuli with random phase (noise) stimuli was repeated for five different values of RMS contrast, in the range from 1.5% to 8.5% (from about twice the visibility threshold for the random phase stimulus to near monitor saturation for the high Michelson contrast line stimulus).

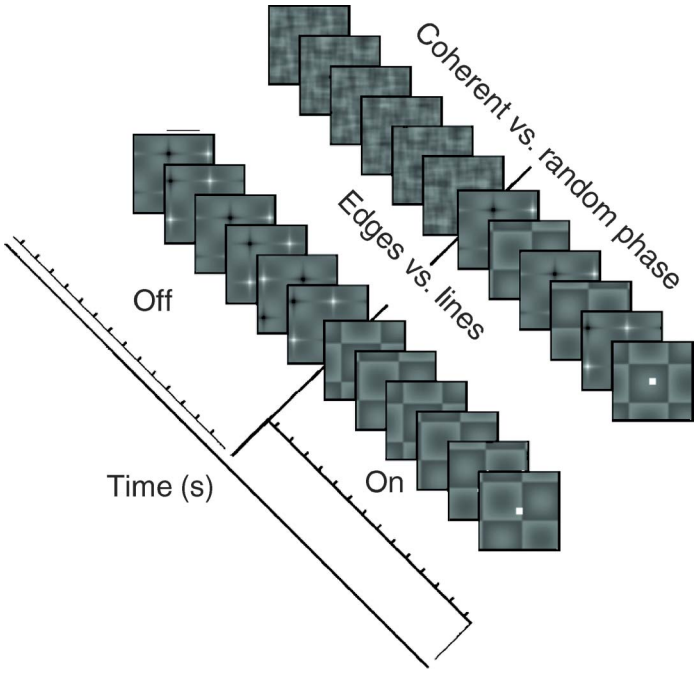

Figure 2. Example of one period of the temporal alternation of the stimuli in the "ON" and "OFF" epochs for the edge versus line condition (left) and coherent phase (edge and line) versus noise condition (right). *Left*: The ON epoch comprised edge stimuli that were displayed at different positions every 2 s, the OFF epoch line stimuli. *Right*: The ON epoch comprised a sequence of randomly intermingled edge and line stimuli, refreshed every 2 s, the OFF epoch comprised a sequence of different noise stimuli, refreshed every 2 s. The vertical bars indicate the times when the stimuli were refreshed (only in offset in the left and both in offset and type in the right). All stimuli (comprising 4 × 3 full periods) were displayed centered around fixation and in a window of 30 × 22.5 deg.

Subjects and procedures

Nine healthy young volunteers (6 males, 3 females) participated to the experiment, up to three MRI recordings. For each recording at least two complete scans for each of the major conditions (alternation between edges versus line stimuli and alternation between phase coherent versus noise stimuli) were collected. For some subjects ten different scanning sessions were run to test the reliability of the responses.

The subjects were instructed to keep fixation to a small gray central fixation point (22.5′ × 22.5′). Fixation was monitored during the experiment by recording ocular movements with the 60-Hz infrared camera equipped in the goggles. The eye movement traces (horizontal and vertical movements and pupil size) were analyzed with Arlington Research Software. The subjects (all experienced

psychophysical observers) never broke fixation, except in one session for one subject that was eliminated from further analysis. In order to control for an attentional modulation of the responses, for two subjects we performed an additional recording session while they were performing a demanding attentional task at fixation point. In these scans the luminance of the fixation point switched from bright to dark and vice versa at random intervals and asynchronously with the 2-s random refresh of the stimuli. The subjects were asked to count the number of fixation point changes. The subjects reported verbally and always correctly the total change number after the end of each scan. For this attentional control each epoch lasted 15 s instead of 30 s.

BOLD responses were acquired by 1.5-T General Electric LX Signa Horizon System (GE, Milwaukee, USA), equipped with Echo-speed gradient coil and amplifier hardware, using a standard quadrature head coil. Activation images were acquired using echoplanar imaging (EPI) gradient-recalled echo sequence (TR/TE/flip angle = 3 s/50 ms/90°, FOV = 280 × 210 mm, matrix = 128 × 128, Acq. Time: 3′12″). Volumes comprised 18 contiguous 4-mm-thick axial slices, covering from the inferior temporal-occipital edge to the middle-parietal region (from about z −28 to 45 mm), acquired every 3 s. Time-course series of 64 images for each volume were collected. The first 12 s of the first epoch, needed to stabilize the signal, was eliminated from any successive analysis. An additional set of anatomical high resolution 3D FastSPGR data set (TR/TE/flip angle = 150 ms/2.3 ms/120°; RBW=12.8 kHz; FOV = 280 × 280 mm, matrix = 256 × 256; isotropic dimension: 1.1 mm, NEX: 2; Acq. Time: 12′26″), was acquired in order to identify subsequent localization of the activation areas and to perform the segmentation and flattening of the brain.

Two types of analysis were performed: for generating a statistical map of the BOLD response, Brain Voyager 2000 4.6 software package (Max-Planck Society, Germany and Brain Innovation, Maastricht, The Netherlands) was used. All volumes from each subject were adjusted with the application of rigid body transforms for residual motion-related signal changes. Functional data were smoothed spatially (Gaussian kernel with a 4-mm full width at half maximum) but not temporally. Statistical activation maps were obtained using cross-correlation analysis thresholding at $p < 0.001$ and clusters of three voxels. Then EPI images were co-registered with the 3D anatomical data in order to define the Talairach–Tournoux coordinates and to generate the flat image of the brain.

As a further quantitative analysis of signals, two regions of interest were selected and a voxel by voxel analysis was performed. The first region of interest comprised the calcarine cortex, anatomically defined from the voxels clearly located in the calcarine sulcus and directly posterior to it, corresponding to the stereotypical anatomical localization of V1 (Hasnain, Fox, & Woldorff, 1998), with little variation across subjects (although we cannot rule the possibility of slight contamination with portions of V2). The second ROI was defined by including all the voxels in associative areas that were active for the alternation of edge vs. line stimulus. These represented a subset of the voxels activated by alternation of both coherent stimuli vs. the noise stimuli. This ROI comprised two foci of activity, one located along the caudal intraparietal sulcus (CIP), and the other along the lateral occipital sulcus (LO), corresponding to the same Talairach coordinates of the areas found with similar stimuli in a previous experiment (see Table 1 and Perna, Tosetti, Montanaro, & Morrone, 2005). Since the two areas were shown to have very similar activity profiles, here we analyze them together in the same ROI.

Having defined for each subject the various ROIs, these were then used to analyze the response of all scans in the same recording session. For each voxel of an ROI the linear trend was calculated and subtracted. Activity was then normalized by the mean of all voxels of the ROI, and the amplitude and phase of the fundamental or second harmonic component of each voxel response in synchrony with the stimulus (expressed in percent of modulation) were calculated. Estimates of amplitude and phase of the response for each ROI were computed from the vectorial average of the single voxels amplitude and phase, with the SE evaluated by the dispersion of the voxel population in the 2-D polar plot (Boynton, Demb, Glover, & Heeger, 1999).

S/N ratio was evaluated by the amplitude of the average response at fundamental frequency, divided by the estimated noise at the same frequency obtained by an exponential fit of the power spectra. The fit was performed only on non-signal harmonics, that is, the harmonics not in synchrony with stimulus alternation (for details, see Boynton et al., 1999).

The ROI time course is the average activity of each normalized voxel, and a similar analysis was performed when the time course was averaged across subjects (in the latter case the average was not weighted by voxel number).

	CIP			dLO		
Subject	*x*	*y*	*z*	*x*	*y*	*z*
AB	34	−80	20	40	−80	10
AP	32	−82	24	43	−75	12
CM	31	−85	21	46	−84	10
CP	39	−79	22	40	−78	10
MA	34	−78	22	45	−70	8
MG	24	−86	24	35	−86	10
SD	27	−81	24	44	−79	11
SB	29	−76	30	42	−85	16
SN	33	−84	22	46	−78	8

Table 1. Talairach coordinates of the two extrastriate foci of activity in response to lines versus edges alternation in the dorsal lateral occipital cortex (dLO) and in the caudal intraparietal sulcus (CIP) of nine subjects.

Local energy modeling

The visual stimuli were convolved with even- and odd-symmetric detectors, having the same amplitude spectra but differing in phase spectra by a constant 90 deg. The phase is chosen so that they have even and odd symmetries for each preferred orientation ϑ.

The filters amplitude spectrum follows a Gaussian function of log spatial frequency (ω, u) approximating the spatial frequency tuning functions of human vision:

$$a(u,\omega) = e^{-\ln^2(|u|/p)/2\cdot s_u^2} \cdot e^{-(\omega-\vartheta)^2/2\cdot s_\omega^2}, \quad (2)$$

where ω is the direction parallel to the preferred orientation and orthogonal to u, and p, S_u, and S_ω are suitably defined constants. The function is a parabola along u on a log–log plot with a peak corresponding to p and a half bandwidth corresponding to S_u log units at half-height. Filters of different sizes and orientations were applied to the visual stimuli (using FFT), and local energy was computed as the Pythagorean sum of the even- and odd-symmetric filter responses.

In the simulation, p varied from 1 to 16 c/deg in steps of one octave and four filter orientations (22.5, 45, 67.5, 90 deg) were used. S_u was equal to 0.55 log units, while orientation selectivity S_ω ranged from ~40 deg for the filter at p = 1 c/deg to 2.6 deg for the filter at p = 16 c/deg, to produce filter with nearly scalable line spread functions.

Results

Alternation of coherent phase stimuli (like the edge stimulus example in Figure 1A and the line stimulus example in Figure 1B) against the random phase stimulus (noise example in Figure 1C) elicited a widespread activity in several visual areas (Figure 3), including calcarine cortex and many extrastriate visual areas. In this condition the stimuli of the ON epoch have, on average, the same Michelson contrast as stimuli used in the OFF epoch and all the stimuli have the same RMS contrasts (see Figure 1). The phase congruency and the local distribution of stimulus energy is different in the ON and OFF phases, the edge and the line stimuli having both higher local energy peaks than noise stimuli used in the rest period (see profiles in Figure 1). The activity along the calcarine sulcus followed the first 1.5–2 cm from the most posterior location of the sulcus, with the dorsal and ventral maximum activity foci (see Figure 3, left) being located midway. To limit the possible contamination from adjacent V2 cortex, we selected only the maximum focus of these activities (one dorsal and one ventral), underestimating dramatically the portion of active V1 to about 19.1 ± 2.3 voxels for each focus (Dougherty et al., 2003).

When the edge stimulus was contrasted against the line stimulus, no activity was found in the calcarine region (both in the central or in the peripheral representation) or in other early retinotopic visual areas (like V3 and V4;

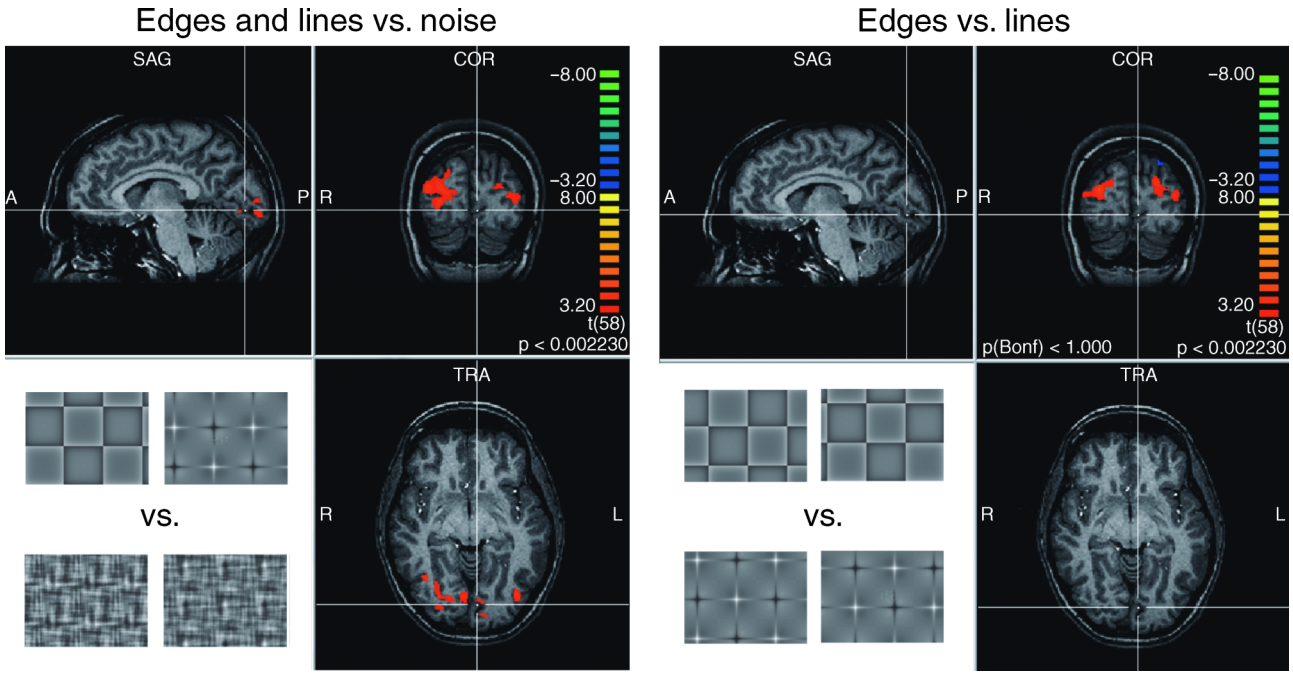

Figure 3. *Left*: Pattern of activity elicited by the alternation of edge and line vs. noise stimuli (stimuli in Figures 1A and 1B vs. Figure 1C) in one subject. *Right*: Response to alternation between edge vs. line stimuli (stimulus in Figure 1A vs. Figure 1B). Alternation of edge vs. line elicits only localized activity in two brain areas, one located in the lateral occipital sulcus and the other in the caudal branch of the intraparietal sulcus. Alternation of edge and line against noise elicits a more widespread activity (stronger for coherent than for random stimuli), including many visual areas, and in particular along the calcarine sulcus.

Figure 3). Differential activation was localized in two higher level visual areas: one region extending along the lateral occipital sulcus, probably including the weakly retinotopic visual areas named dorsal LOC and the other in the more caudal part of the occipital branch of the intraparietal sulcus (Figure 3). The lack of a pervasive response to alternation of the edge stimulus against the line stimulus is surprising, since the two stimuli, in spite of having the same local- and global-energy distribution, are perceptually clearly different and have extremely different values of Michelson contrasts. In addition the edge stimulus, a missing-fundamental checkerboard, elicits an illusion of brightness/darkness that fills in the center of each square, not elicited by the line stimulus.

The two foci of differential activity correspond well to the same Talairach localizations obtained by Perna et al. (2005) with stimuli eliciting Craik–O'Brian illusion (see Table 1). However for the present stimuli the response was more extensive and often the two clusters merged in one. For this reason, here we combined the analyses of the two clusters in a single ROI.

For each subject, we defined two ROIs (using Brain Voyager) based on the response to the two combinations of stimuli with different phase congruency: one that extended along the calcarine sulcus (based on the response to coherent phase versus noise stimuli) and one that extended along the union of the LO and CIP (based on the response to edge versus line stimuli). Given that the two different scans were repeated several times for each subject and for different scanning sessions, we always verified the consistence between the locations of the ROIs and the responses for each subject. On these ROIs we performed a single voxel analysis in response to both the localizer and the remaining stimuli alternation. The analysis of the individual subjects is the average (or scatter) of all responses. The single voxel analysis was performed to validate the absence of a weak and distributed response to stimuli differing in phase value that could be missed with the conservative threshold used for Brain Voyager. Figure 4 reports the BOLD signal modulation in the calcarine region ROI (upper row) and dLO + CIP ROI (lower row), averaged over all the subjects participating in the experiment. The left column shows the responses to the alternation of coherent phase against noise stimuli (Figures 1A and 1B vs. Figure 1C), while the right one shows the response to the alternation of edge stimuli against line stimuli (Figure 1A vs. Figure 1B).

While activity inside the calcarine ROI shows a strong and robust modulation in synchrony with the alternation of coherent phase stimuli versus noise stimuli, no signal modulation was found for the same voxels when the edge stimulus was presented against the line stimulus. A different behavior was observed for the associative cortex ROI. LO-CIP ROI shows a strong modulation in phase with stimulus presentation for both conditions. Note also that the response to phase congruency does not increase from primary to associative cortex.

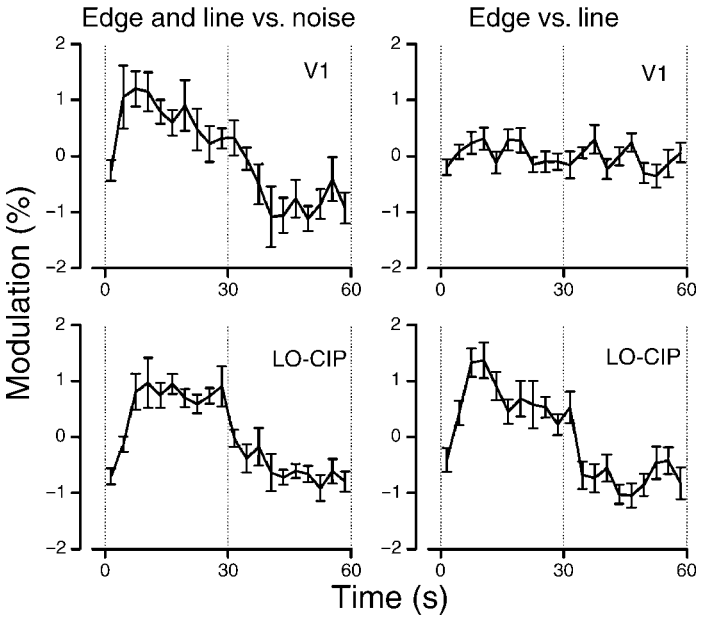

Figure 4. Time courses of BOLD responses averaged across all the subjects for the primary visual cortex ROI (upper row) and the union of the dLO and CIP ROI (lower row). The left column shows the response to edge and line vs. noise stimuli, the right column to the alternation of edge versus line stimuli. The bars represent ±1 *SE* of the mean. The dashed lines show the time of stimulus transition. Note the absence of response to the alternation of line versus edge stimuli, despite the same ROI show a strong response to alteration of coherent vs. random stimuli.

To quantify the effect and to be certain of the absence of edge–line specific responses in primary visual cortex, Figure 5 plots for each subject the amplitude (open circles, top row) and the associated signal-to-noise ratio (open triangles, bottom row) of the response of edge vs. line stimuli (Figures 5A, 5C, 5E, and 5G) and the response of edge and line vs. noise stimuli (Figures 5B, 5D, 5F, and 5H). Each symbol represents a single subject, with both conditions measured in the same scan session. The angular position is the mean phase of fundamental harmonic for all the voxels in the ROI. Phase values near 90 degrees mean that neuronal activity is in synchrony with the ON epoch of the visual stimuli; a phase value of 270 degrees indicates a stronger response to the OFF epoch than to the ON epoch. Response phases slightly different from these values may be the consequence of the hemodynamic shift or adaptation of BOLD signal (Boynton, Engel, Glover, & Heeger, 1996). The responses of primary cortex (Figures 5B and 5F) were all strong for the stimuli varying in phase congruency but virtually non-existent for stimuli differing in absolute phase, often with S/N ratios below 1 and amplitude with large standard error not significantly different from zero. The responses in CIP and LO (Figures 5C, 5D, 5G, and 5H) were quite different: the combined responses of those areas to stimuli differing in absolute phase (edges alternated with lines)

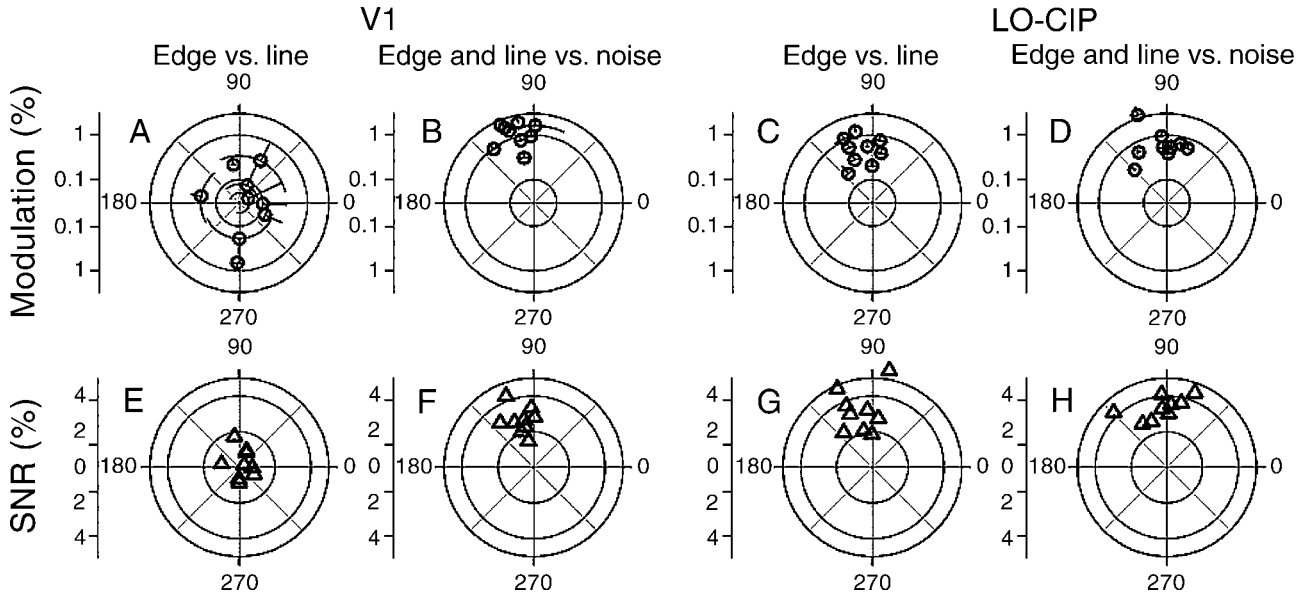

Figure 5. Polar plot of the amplitude and phase of the fundamental harmonic of the BOLD response, with associated *SEM* (first row) and S/N ratio (second row) of all individual subjects for the two stimulus conditions and in the two ROIs. The labels in the top refer to the stimuli illustrated in Figure 1. The RMS contrast of the stimuli was equal to 4.25%.

were similar to those differing in congruency, both in reliability (S/N) and in amplitude. The responses of CIP and dLO were also analyzed separately and found to be very similar, so here we show only the combined data.

For stimuli differing in phase congruency (edge and line versus noise) we also tested dependency of the BOLD responses on the RMS contrast of the stimuli (the RMS contrast value was the same during the ON and OFF epochs). The plot of Figure 6 reports the amplitude of the modulation of the individual ROI averaged between subjects as a function of RMS contrast. At medium and low contrasts, response to edge and line stimuli is higher than response to noise stimuli both in the calcarine and in the dLO − CIP ROI (all the values of modulation are positive). However, at the higher contrast tested, the preference for coherent stimuli, shown by the BOLD signal, was strongly reduced. dLO − CIP ROI shows a similar preference for coherent stimuli over noise stimuli, which seems to be stable at a wide range of contrast values. The various lines represent the predictions of a local energy model associated to a non-linear response gain explained in detail in the Methods section and in the following.

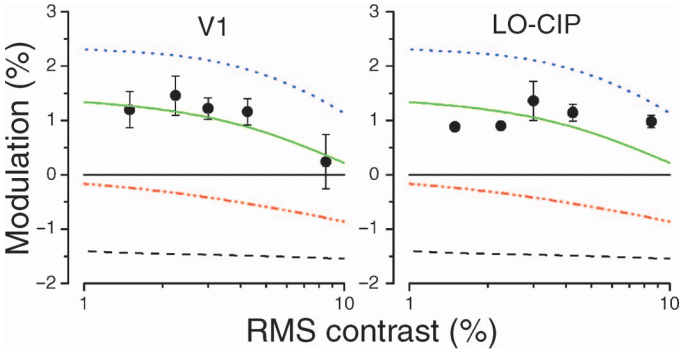

Figure 6. Amplitude of BOLD signal modulation in primary visual cortex and dLO and CIP ROI projected along the stimulus direction as a function of RMS stimulus contrast for the alternation of the edge and line vs. noise, averaged across subjects. The lines are prediction of a local energy model with a non-linear response gain given by Equation 4. The curves correspond to different values of the β exponent equal to 1, 2, 3, and 4 from bottom to top. The continuous green curve correspond to $\beta = 3$.

The local energy E_S at each image location is obtained by the Pythagorean sum of the outputs of the even- and odd-symmetric receptive fields (S_E and S_O) for each given orientation and spatial frequency preferences (see Methods section):

$$E_S = \sqrt{S_E^2 + S_O^2}. \quad (3)$$

The Local Energy function E_S and its square power (E_S^2) function is invariant with absolute phase, consistent with the invariance observed in the data for primary visual cortex. However, the two functions predict different responses to coherent versus noise stimuli: E_S^2 power function would predict a lack of response to phase congruency (for Parseval theorem), while this is not the case for the E_S energy function that would generate a larger average response (over space) to noise stimuli than to coherent phase stimuli, as can be observed in Figure 7A.

Coherent stimuli (Figure 7A, red curves) have near zero energy everywhere, except at the locations of image features (edges or lines), where the energy profile shows

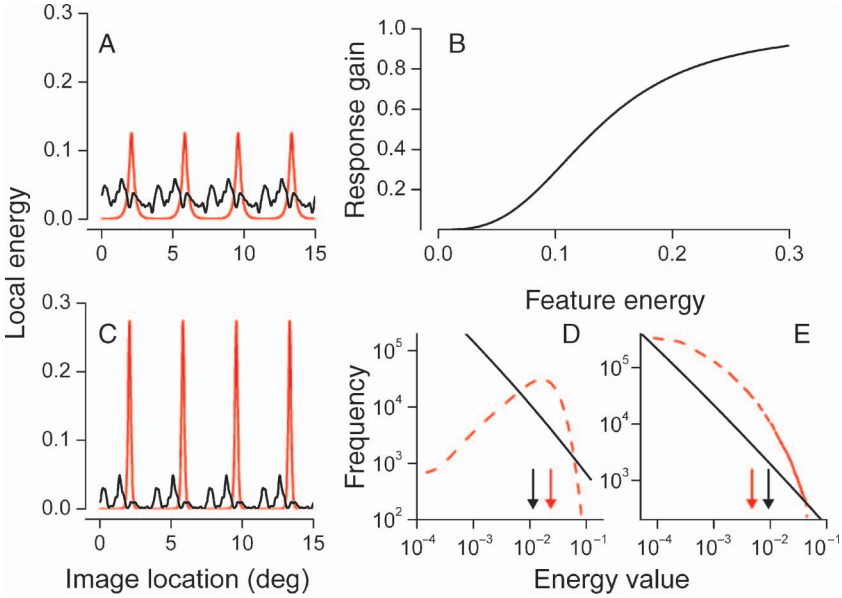

Figure 7. (A) Example of local energy function in response to a particular row of the coherent phase (black) and to noise stimuli (red). (B) Example of the non-linear response gain function applied after the computation of the local energy, given by Equation 4 with β equal to 3. (C) The local energy response of profiles in (A) after the non-linear gain stage with $\beta = 3$. (D) Local energy distribution of coherent (black continuous curve) and noise (red dashed curve) stimuli computed for all positions and filter selectivities. The arrow illustrates the mean response to random phase (red) and coherent phase (black) stimuli. (E) Distribution of the local energy after the non-linear gain with $\beta = 3$. The average response to coherent phase (black arrow) is greater than the average response to noise stimuli.

sharp spatial peaks. On the other hand, noise stimuli present a more uniform distribution of energy across space. The distributions of the E_S energy values for the congruent (red) and the noise stimuli (black; computed for all stimulus positions, orientations, and spatial frequency selectivity of the input filters) is reported in Figure 7D. The frequency distributions for the coherent and noise stimuli are very different. For coherent phase stimuli, the most frequent energy value is zero with a roughly linear decay of probability with energy values (black curve); in random stimuli, the distribution is peaked around average values of local energy (red dashed curve). If the BOLD response correlates with the average energy response (the integral of all local energy values weighted with their frequency in the image, indicated by the red and black arrows), a higher response to the random patterns would be predicted.

So both the energy and the power function predictions are not verified by the V1 activity that shows a stronger response to coherent phase stimuli for a wide range of stimulus contrasts. In addition both functions would predict that the response should be constant at all contrast values. Also this prediction is false, given that the activity of V1 to coherent stimuli declines with contrast.

To simulate the greater response to coherent phase than random phase stimuli of V1, the weight associated with the higher energy values should be increased. This can be obtained by applying an expansive transducer response function.

We assumed that neural response is related to the local energy of the visual stimulus through a gain function (Figure 7B) given by

$$\underset{\theta,\omega}{R} = \alpha \cdot \sum_{S} \frac{E_S^{\beta}}{E_S^{\beta} + g_0^{\beta}}, \tag{4}$$

where R is the neural activity at one spatial scale and orientation, E_S is the local energy (Equation 3) corresponding to a given position in the image for the given spatial frequency and orientation, and g_0 is a semi-saturation constant. In our simulation we fixed g_0 to one half the maximum of local energy computed for stimuli at the higher contrast.

The gain function introduces a non-linearity (whose strength is encoded by the parameter β of Equation 4) that amplifies the effect of energy maxima on neuronal response. For example, the peaks of the profile in Figure 7A are strongly amplified by applying the non-linear gain with exponent β equal to 3 (Figure 7C), inducing a change in the frequency distribution functions. Figure 7E shows the distributions obtained with β equal to 3: with this exponent the frequency distribution of the random phase stimuli changes shape, shifting at lower energy values, while that of the congruent phase stimuli shifts toward higher energy values. The net effect is that the average values of the energy after the non-linear gain are higher for the congruent phase stimuli than for the random phase stimuli.

The results of the simulation are shown together with the experimental data in Figure 6. For low values of exponent β (namely 1, dash black curve, or 2, dash-dot-dot red curve), a stronger BOLD signal for the random phase pattern than for coherent stimuli is obtained. Only an exponent of three or more can explain the function of BOLD signal versus contrasts and the higher response to stimuli A and B than to stimulus C. Different values of parameter α can multiplicatively affect the curves, shifting in vertical dimension, but cannot invert the sign. Different values of the parameter g (semi-saturating energy) shift the curve along the horizontal axis. For V1 responses, the best fit of the dependence of the BOLD modulation with contrast is obtained for $\beta = 3$ (continuous green curve).

The model prediction of the dLO + CIP responses is not very satisfactory, given these areas do not show a strong dependence on contrast. A good simulation could be obtained by applying an additional response gain stage (Equation 4) to the output of V1 responses. However, these areas are also able to discriminate between the different coherent phase values, indicating that they might perform a qualitatively different analysis, like the synthesis of the form or structure of the image from the individual feature (see Discussion section).

Attentional control

The result that noise stimuli elicit a weaker BOLD response than coherent phase stimuli could in principle reflect a modulation by attention. It is possible that highly structured stimuli attract more attention and this may result in a greater activation (Tootell et al., 1998). To assure that attentional resources are equally engaged for the two types of stimuli, in two subjects we recorded the activity while they were performing a demanding counting task that required sustained attention allocated to the fixation target. Figure 8 reports the average activity measured in the same scan session for the alternation of the coherent phase stimuli versus the random noise in normal condition and when the fixation target changed contrast polarity between 20 and 30 times. The subjects correctly reported the polarity alternations. Nevertheless the BOLD response both in V1 and in dLO + CIP did not change significantly between the two conditions, indicating the absence of a strong attentional modulation in these areas.

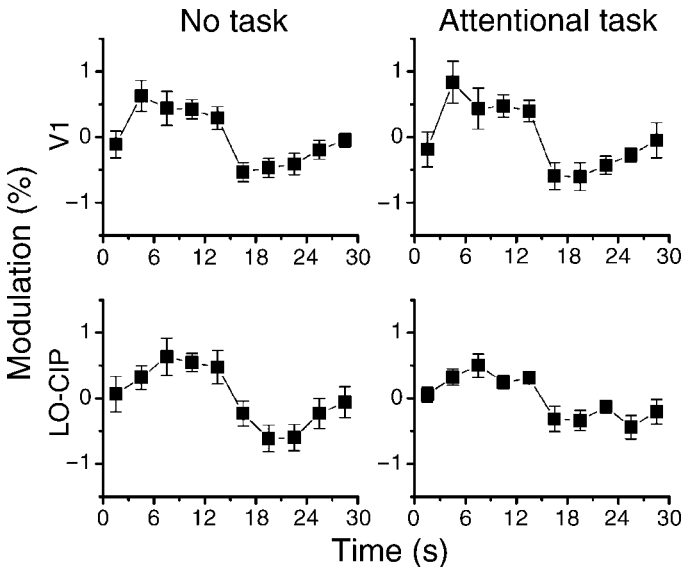

Figure 8. Time courses of BOLD responses averaged across two subjects for the primary visual cortex ROI (upper row) and the union of the dLO and CIP ROI (lower row) in response to edge and line vs. noise stimuli. In the left columns, the subjects passively observed the stimuli, in the right they were performing a demanding counting task at fixation.

Discussion

We recorded the BOLD response to visual stimuli that have the same power spectrum (hence the same RMS contrast) but different Michelson contrasts and different congruence of phase across harmonics. Primary visual cortex always responded more strongly to stimuli with coherent phase than to random stimuli but responded equally to stimuli with the same local energy distribution (i.e., the same phase congruency pattern between the harmonics) such as the line or the edge stimuli. Differences in the Michelson contrast of the stimuli cannot explain these results. A clear activation of primary visual cortex was observed when alternating the line and edge stimuli against random stimuli, a condition where the two epochs have, on average, the same Michelson contrast. On the other hand, no activity was measurable in primary visual cortex for the alternation of the line versus edge stimuli, despite the fact that these two stimuli differ by more than a factor of five in Michelson contrast.

Similarly, RMS contrast cannot account for BOLD signal modulation: all the stimuli used in the experiment had exactly the same RMS contrast at any spatial or orientation band but elicited different neuronal activities. Nor can the differences in BOLD activity be ascribed to attenuation of some spatial frequencies by the contrast sensitivity mechanisms, given that the stimuli had the same frequency amplitude spectra. Nor to a greater attentional allocation to the coherent stimuli, given that in the condition where attention is allocated to a central task, a similar modulation was observed.

These conclusions are valid for a wide range of contrasts, from twice to ten times the detection threshold. However, there is a clear decrease, in all subjects, of the preference for the phase coherent stimuli in V1 for high contrast values. These results indicate that coherence between harmonic components is analyzed or computed

in primary visual cortex, but that the particular phase value (line or edge) is not represented at population level.

Based on the dependence of the preference for phase congruency as a function of contrast, we propose a simple model of neuronal response involving computation of local energy (Burr & Morrone, 1992; Morrone & Burr, 1988; Morrone & Owens, 1987) and a non-linear response gain function that can account for the present data and the discrepant results in the literature. There is clear evidence that the contrast response function of primary visual cortex is not linear but modulated by gain contrast mechanisms. For stationary conditions, when prevailing contrast does not change rapidly over time, the simplest way to account for the action of gain mechanisms is to consider a sigmoidal response function. Psychophysical experiments (Foley, 1994; Legge & Foley, 1980), measurements of electrophysiological contrast responses (Albrecht & Hamilton, 1982; Carandini, Heeger, & Movshon, 1997; Finn, Priebe, & Ferster, 2007; Sclar, Maunsell, & Lennie, 1990), and fMRI contrast responses (Boynton et al., 1999; Olman et al., 2004) all indicate that an exponent of between 2 and 3 can provide a good fit to the experimental data. We simulated the mechanism by assuming a non-linear response of the individual local energy operators. To simulate the present data, it is necessary that the exponent is around 3, in agreement with previous evidence. It is worthwhile noting that to simulate the phase congruency selectivity it is not essential to apply the gain transducer function to the energy, but any non-linear response function of the individual linear neuronal RFs with various symmetry could equally well simulate the data. However, such a model would have difficulties in explaining the invariance with phase value and might simulate it only for very specific conditions (like RF with all forms of symmetry represented with equal strength). The local energy model is particularly useful in localizing important features for image segmentation, implementing a great reduction of redundant or irrelevant information. This is achieved by retaining only information that corresponds to local maxima (point of maximum phase congruency). It is worthwhile noting that accelerating gain responses would facilitate the localization of the maxima of the energy, particularly for low contrast images.

Many studies have compared human BOLD activity in response to natural images and to scrambled images (Epstein & Kanwisher, 1998; Grill-Spector et al., 1998; Kanwisher et al., 1997; Kourtzi & Kanwisher, 2000; Rainer et al., 2002), the most common result being a preference of primary visual cortex for highly scrambled images. In anesthetized monkey, Rainer et al. (2002) found that for moderate levels of scrambling the preference is for natural images and explained the preference to scrambling to the presence of spurious spatial frequency and the action of the contrast sensitivity function. Only a few previous studies have investigated the dependency of primary visual cortex activity on phase coherence. Rainer et al. (2001) in monkey studied how random perturbation of natural image phase spectra modulated the BOLD response. In agreement with the present study, V1 response was greater for the natural image than for the random phase image. The exact dependence on phase scrambling, however, could not be derived for a technical error in blending the phase coherent with the phase incoherent images (see Dakin et al., 2002).

Olman et al. (2004), at odds with the results of the previous authors, found that the BOLD signal in primary visual cortex is insensitive to phase manipulation of natural images. These authors also find that the RMS contrast is the important factor in eliciting a BOLD modulation. At first sight this result may appear to contradict the present data, but it does not. Although a quantitative comparison between their results—based on natural image presentation—and ours—using highly coherent synthetic stimuli—is not possible, the model used to simulate our data can explain the Olman et al. results. The RMS contrast values used by these authors in the natural images and noise response measurements were much higher than those used in our experiment. In addition, the contrast response function calculated by the same authors for their stimuli showed a compressive non-linearity, suggesting that the stimuli used by these authors are in the saturating part of the energy gain function, where our model predicts a small or null difference between coherent and noise patterns. More recently the effect of random phase perturbation has been investigate by Tjan et al. (2006). These authors find that about half of their subjects preferred natural images to random (but the preference was very slight). Unfortunately the RMS contrast of the images has not been reported and hence it is difficult to assess if a similar explanation could apply to this study.

In addition to the RMS contrast dependence, three other factors may have obscured the preference for natural images in these studies. First, the phase congruency of natural images is never total, as it is in our artificial stimuli, and this would generate a smaller BOLD modulation between the random and natural images. Secondly, our stimuli did not contain low spatial frequencies, while these spatial frequencies have high amplitudes in natural images (Olshausen & Field, 1996). Low spatial frequencies are likely to be less influenced from phase congruency than higher spatial components, since the low spatial frequency detectors respond to a single or few spatial harmonics given the filter bandwidth scales with spatial frequencies. Thirdly, the overall contrast of our stimuli was always constant through each scan, while the necessity to perform the psychophysical task in these previous studies imposed that the images were transiently presented against a blank field. Transient and large increase of contrast may amplify non-linear components of the BOLD response masking the selectivity for phase congruency. In addition, if the increased BOLD response for phase-coherent stimuli involves processes such as

non-classical receptive field modulation, it is possible that these effects are stronger with our more regular stimuli than with the natural images used by these authors.

The preference for phase-coherent stimuli is supported by single neuron activity of area 17. Felsen et al. (2005, Touryan et al., 2005) registered the neuronal responses to features presented in either natural images or noise stimuli and found a higher response to features in natural images for complex cells but not for simple cells. Interestingly, complex cell response was more sensitive to manipulation of phase congruency than to amplitude spectra. It would be interesting to test if the different responses in the complex cell could be derived by a non-linear gain modulation applied to the energy computation.

Response gain in the cortex is strongly modulated by the presence of energy at different orientations. Cross-orientation inhibition (Bonds, 1989; Carandini et al., 1997; DeAngelis, Robson, Ohzawa, & Freeman, 1992; Morrone & Burr, 1986; Morrone, Burr, & Maffei, 1982; Shapley, Hawken, & Ringach, 2003; Somers, Nelson, & Sur, 1995) may be the mechanism generating the differential response between different phase-coherence stimuli, given that locally the orientation distribution of the energy in the random phase stimuli is more constant at all spatial position (Morgan et al., 1991). Gain modulation could also result from mechanisms of long range or contextual modulation, including suppressive modulation in the random stimuli and non-classical receptive field enhancement in the phase-coherent stimuli. Interestingly, however, any mechanism of contextual modulation improving the saliency of relevant visual features should act in a similar way for edges and lines, given the lack of a BOLD response to alternation between line and edge stimuli. Edge and line stimuli, besides having the same spatial structure, appear perceptually very different from each other, with the edge stimuli producing a strong brightness illusion. Each square appears dark or light depending on the edge polarity (although it has the same physical luminance), as it happens in Cornsweet illusion. The lack of BOLD discrimination between these stimuli supports early evidence (Cornelissen, Wade, Vladusich, Dougherty, & Wandell, 2006; Perna et al., 2005) that brightness is not explicitly computed in primary visual cortex.

The lack of differential activity between line and edge stimuli suggests that there exists in primary visual cortex both even-symmetric and odd-symmetric classes of detectors and that the two classes are equally represented. A single class of receptors (being the even- or odd-symmetric receptive field) will respond differently to edge stimuli than to line stimuli. However the differential responses are expected to be small at the level of the neuronal population activity, due to averaging across image locations. Psychophysical and VEP experiments (Burr, Morrone, & Fiorentini, 1992; Burr et al., 1989), as well as electrophysiological data on monkey primary visual cortex (Ringach, 2002), indicate a balanced representation of even- and odd-symmetric detectors. However, the invariance of the response with the phase of the stimuli does not exclude the possibility that there exist neurons with receptive fields that code efficiently intermediate phases, but if they exist they should be equally represented as suggested by electrophysiology recordings (Field & Tolhurst, 1986; Gaska et al., 1987; Jones & Palmer, 1987; Pollen et al., 1988).

Two recent studies have measured directly the selectivity to phase of compound gratings (Mechler et al., 2002, 2007). These studies used stimuli that have maximum phase congruency, like those used in the present study. Both complex and simple cells are tuned to phase, with an even distribution. Interestingly, at the population level, the neuronal responses do not code phases with the high sensitivity attained by human performance. This result is in agreement with the invariance of the BOLD response for phase that we found in V1, shown by the lack of activity for edges vs. line presentation. Also the illusory brightness difference induced by edges has no effect on V1 BOLD response, suggesting that contextual modulation of response to local features and filling in of surface brightness are performed at different levels of image analysis and perhaps rely on different neuronal mechanisms.

Two higher order brain areas, located along the lateral occipital sulcus and in the caudal part of the intraparietal sulcus, were activated by the alternation of edge and line stimuli, showing a stronger activity for the former than for the latter. The Talairach localizations of these areas were consistent with those found in our previous study (Perna et al., 2005) and thought to be involved in the computation of apparent brightness. It is possible that the origin of the response is related to the lightness or darkness illusion induced by the missing-fundamental checkerboard of the edge stimulus. However, we cannot exclude the possibility that the response is related to a real decoding of phase and feature types (such as an unbalanced number of even and odd receptive fields), or to a preference to complex image characteristics including stimulus symmetry (Sasaki, Vanduffel, Knutsen, Tyler, & Tootell, 2005) and segmentation in planar surfaces (Tsutsui, Sakata, Naganuma, & Taira, 2002). These areas can be anatomically assigned to the dorsal part of the lateral occipital complex, a large non-retinotopic visual area functionally defined from the stronger response to objects than to scrambled objects (Kourtzi & Kanwisher, 2000). Interestingly, the group of voxels activated by alternation of edge and line stimuli vs. their random phase version forms a subset of the object selective area (Tjan et al., 2006), suggesting the existence of several foci in dLO that can discriminate structured versus unstructured scenes.

In conclusion, the present data suggest that the human primary visual cortex is sensitive to phase congruency but invariant to the phase (edge or line) of the stimulus feature. Two areas of the dorsal stream are able to classify image type (edge or line) and hence may mediate the reconstruction of surfaces from sparse local information.

Acknowledgments

We are grateful to David Burr for helpful comments in the manuscript and to Laura Biagi for help during the data analysis. This research was supported by MIUR PRIN grants and by ERC grant STANIB.

Commercial relationships: none.
Corresponding author: Maria Concetta Morrone.
Email: concetta.morrone@inpe.unipi.it.
Address: Department of Human Physiology "G Moruzzi," University of Pisa, Via S Zeno 31, 56127 Pisa, Italy.

References

Adelson, E. H., & Bergen, J. R. (1985). Spatiotemporal energy models for the perception of motion. *Journal of the Optical Society of America A, Optics and Image Science, 2,* 284–299. [PubMed]

Albrecht, D. G., & Hamilton, D. B. (1982). Striate cortex of monkey and cat: Contrast response function. *Journal of Neurophysiology, 48,* 217–237. [PubMed]

Bonds, A. B. (1989). Role of inhibition in the specification of orientation selectivity of cells in the cat striate cortex. *Visual Neuroscience, 2,* 41–55. [PubMed]

Boynton, G. M., Demb, J. B., Glover, G. H., & Heeger, D. J. (1999). Neuronal basis of contrast discrimination. *Vision Research, 39,* 257–269. [PubMed]

Boynton, G. M., Engel, S. A., Glover, G. H., & Heeger, D. J. (1996). Linear systems analysis of functional magnetic resonance imaging in human V1. *Journal of Neuroscience, 16,* 4207–4221. [PubMed] [Article]

Burr, D. C. (1980). Sensitivity to spatial phase. *Vision Research, 20,* 391–396. [PubMed]

Burr, D. C., & Morrone, M. C. (1992). A non-linear model of feature detection. In R. B. Pinter & N. Nabet (Eds.), *Non-linear vision* (pp. 309–328). New York: CRC Press.

Burr, D. C., Morrone, M. C., & Fiorentini, A. (1992). Electro-physiological investigation of edge-selective mechanisms of human vision. *Vision Research, 32,* 239–247. [PubMed]

Burr, D. C., Morrone, M. C., & Spinelli, D. (1989). Evidence for edge and bar detectors in human vision. *Vision Research, 29,* 419–431. [PubMed]

Carandini, M., Heeger, D. J., & Movshon, J. A. (1997). Linearity and normalization in simple cells of the macaque primary visual cortex. *Journal of Neuroscience, 17,* 8621–8644. [PubMed] [Article]

Cornelissen, F. W., Wade, A. R., Vladusich, T., Dougherty, R. F., & Wandell, B. A. (2006). No functional magnetic resonance imaging evidence for brightness and color filling-in in early human visual cortex. *Journal of Neuroscience, 26,* 3634–3641. [PubMed] [Article]

Dakin, S. C., Hess, R. F., Ledgeway, T., & Achtman, R. L. (2002). What causes non-monotonic tuning of fMRI response to noisy images? *Current Biology, 12,* R476–R477. [PubMed] [Article]

DeAngelis, G. C., Robson, J. G., Ohzawa, I., & Freeman, R. D. (1992). Organization of suppression in receptive fields of neurons in cat visual cortex. *Journal of Neurophysiology, 68,* 144–163. [PubMed]

Dougherty, R. F., Koch, V. M., Brewer, A. A., Fischer, B., Modersitzki, J., & Wandell, B. A. (2003). Visual field representations and locations of visual areas V1/2/3 in human visual cortex. *Journal of Vision, 3*(10):1, 586–598, http://journalofvision.org/3/10/1/, doi:10.1167/3.10.1. [PubMed] [Article]

Emerson, R. C., Korenberg, M. J., & Citron, M. C. (1992). Identification of complex-cell intensive nonlinearities in a cascade model of cat visual cortex. *Biological Cybernetics, 66,* 291–300. [PubMed]

Epstein, R., & Kanwisher, N. (1998). A cortical representation of the local visual environment. *Nature, 392,* 598–601. [PubMed]

Felsen, G., Touryan, J., Han, F., & Dan, Y. (2005). Cortical sensitivity to visual features in natural scenes. *PLoS Biology, 3,* e342. [PubMed] [Article]

Field, D. J., & Nachmias, J. (1984). Phase reversal discrimination. *Vision Research, 24,* 333–340. [PubMed]

Field, D. J., & Tolhurst, D. J. (1986). The structure and symmetry of simple-cell receptive-field profiles in the cat's visual cortex. *Proceedings of the Royal Society of London B: Biological Sciences, 228,* 379–400. [PubMed]

Finn, I. M., Priebe, N. J., & Ferster, D. (2007). The emergence of contrast-invariant orientation tuning in simple cells of cat visual cortex. *Neuron, 54,* 137–152. [PubMed] [Article]

Foley, J. M. (1994). Human luminance pattern-vision mechanisms: Masking experiments require a new model. *Journal of the Optical Society of America A, Optics, Image Science, and Vision, 11,* 1710–1719. [PubMed]

Gaska, J. P., Jacobson, L. D., Chen, H. W., & Pollen, D. A. (1994). Space-time spectra of complex cell filters in the macaque monkey: A comparison of results obtained with pseudowhite noise and grating stimuli. *Visual Neuroscience, 11,* 805–821. [PubMed]

Gaska, J. P., Pollen, D. A., & Cavanagh, P. (1987). Diversity of complex cell responses to even- and odd-symmetric luminance profiles in the visual cortex of

the cat. *Experimental Brain Research, 68,* 249–259. [PubMed]

Grill-Spector, K., Kushnir, T., Hendler, T., Edelman, S., Itzchak, Y., & Malach, R. (1998). A sequence of object-processing stages revealed by fMRI in the human occipital lobe. *Human Brain Mapping, 6,* 316–328. [PubMed]

Hasnain, M. K., Fox, P. T., & Woldorff, M. G. (1998). Intersubject variability of functional areas in the human visual cortex. *Human Brain Mapping, 6,* 301–315. [PubMed]

Hubel, D. H., & Wiesel, T. N. (1962). Receptive fields, binocular interaction and functional architecture in the cat's visual cortex. *The Journal of Physiology, 160,* 106–154. [PubMed] [Article]

Hyvärinen, A., & Hoyer, P. O. (2001). A two-layer sparse coding model learns simple and complex cell receptive fields and topography from natural images. *Vision Research, 41,* 2413–2423. [PubMed]

Jones, J. P., & Palmer, L. A. (1987). The two-dimensional spatial structure of simple receptive fields in cat striate cortex. *Journal of Neurophysiology, 58,* 1187–1211. [PubMed]

Kanwisher, N., McDermott, J., & Chun, M. M. (1997). The fusiform face area: A module in human extrastriate cortex specialized for face perception. *Journal of Neuroscience, 17,* 4302–4311. [PubMed] [Article]

Kourtzi, Z., & Kanwisher, N. (2000). Cortical regions involved in perceiving object shape. *Journal of Neuroscience, 20,* 3310–3318. [PubMed] [Article]

Kovesi, P. (1999). Image features from phase congruency. *Videre: A Journal of Computer Vision Research* (vol. 1). MIT Press.

Legge, G. E., & Foley, J. M. (1980). Contrast masking in human vision. *Journal of the Optical Society of America, 70,* 1458–1471. [PubMed]

Martini, P., Girard, P., Morrone, M. C., & Burr, D. C. (1996). Sensitivity to spatial phase at equiluminance. *Vision Research, 36,* 1153–1162. [PubMed]

Mechler, F., Ohiorhenuan, I. E., & Victor, J. D. (2007). Speed dependence of tuning to one-dimensional features in V1. *Journal of Neurophysiology, 97,* 2423–2438. [PubMed] [Article]

Mechler, F., Reich, D. S., & Victor, J. D. (2002). Detection and discrimination of relative spatial phase by V1 neurons. *Journal of Neuroscience, 22,* 6129–6157. [PubMed] [Article]

Morgan, M. J., Ross, J., & Hayes, A. (1991). The relative importance of local phase and local amplitude in patchwise image reconstruction. *Biological Cybernetics, 65,* 113–119.

Morrone, M. C., & Burr, D. C. (1986). Evidence for the existence and development of visual inhibition in humans. *Nature, 321,* 235–237. [PubMed]

Morrone, M. C., & Burr, D. C. (1988). Feature detection in human vision: A phase-dependent energy model. *Proceedings of the Royal Society of London B: Biological Sciences, 235,* 221–245. [PubMed]

Morrone, M. C., & Burr, D. C. (1997). Capture and transparency in coarse quantized images. *Vision Research, 37,* 2609–2629. [PubMed]

Morrone, M. C., Burr, D. C., & Maffei, L. (1982). Functional implications of cross-orientation inhibition of cortical visual cells. I. Neurophysiological evidence. *Proceedings of the Royal Society of London B: Biological Sciences, 216,* 335–354. [PubMed]

Morrone, M. C., Burr, D. C., & Ross, J. (1994). Illusory brightness step in the Chevreul illusion. *Vision Research, 34,* 1567–1574. [PubMed]

Morrone, M. C., Burr, D. C., & Spinelli, D. (1989). Discrimination of spatial phase in central and peripheral vision. *Vision Research, 29,* 433–445. [PubMed]

Morrone, M. C., & Owens, R. (1987). Feature detection from local energy. *Pattern Recognition Letters, 1,* 103–113.

Morrone, M. C., Ross, J., Burr, D. C., & Owens, R. (1986). Mach bands depend on spatial phase. *Nature, 324,* 250–253.

Movshon, J. A., Thompson, I. D., & Tolhurst, D. J. (1978a). Receptive field organization of complex cells in the cat's striate cortex. *The Journal of Physiology, 283,* 79–99. [PubMed] [Article]

Movshon, J. A., Thompson, I. D., & Tolhurst, D. J. (1978b). Spatial summation in the receptive fields of simple cells in the cat's striate cortex. *The Journal of Physiology, 283,* 53–77. [PubMed] [Article]

Olman, C. A., Ugurbil, K., Schrater, P., & Kersten, D. (2004). BOLD fMRI and psychophysical measurements of contrast response to broadband images. *Vision Research, 44,* 669–683. [PubMed]

Olshausen, B. A., & Field, D. J. (1996). Natural image statistics and efficient coding. *Network, 7,* 333–339. [PubMed]

Openheim, A. V., & Lim, J. S. (1981). The importance of phase in signals. *Proceedings of the IEEE, 69,* 529–541.

Perna, A., & Morrone, M. C. (2007). The lowest spatial frequency channel determines brightness perception. *Vision Research, 47,* 1282–1291. [PubMed]

Perna, A., Tosetti, M., Montanaro, D., & Morrone, M. C. (2005). Neuronal mechanisms for illusory brightness

perception in humans. *Neuron, 47,* 645–651. [PubMed] [Article]

Piotrowski, L. N., & Campbell, F. W. (1982). A demonstration of the visual importance and flexibility of spatial-frequency amplitude and phase. *Perception, 11,* 337–346. [PubMed]

Pollen, D. A., Gaska, J. P., & Jacobson, L. D. (1988). Responses of simple and complex cells to compound sine-wave gratings. *Vision Research, 28,* 25–39. [PubMed]

Rainer, G., Augath, M., Trinath, T., & Logothetis, N. K. (2001). Nonmonotonic noise tuning of BOLD fMRI signal to natural images in the visual cortex of the anesthetized monkey. *Current Biology, 11,* 846–854. [PubMed] [Article]

Rainer, G., Augath, M., Trinath, T., & Logothetis, N. K. (2002). The effect of image scrambling on visual cortical BOLD activity in the anesthetized monkey. *Neuroimage, 16,* 607–616. [PubMed]

Ringach, D. L. (2002). Spatial structure and symmetry of simple-cell receptive fields in macaque primary visual cortex. *Journal of Neurophysiology, 88,* 455–463. [PubMed] [Article]

Ringach, D. L. (2004). Mapping receptive fields in primary visual cortex. *The Journal of Physiology, 558,* 717–728. [PubMed] [Article]

Ross, J., Morrone, M. C., & Burr, D. C. (1989). The conditions under which Mach bands are visible. *Vision Research, 29,* 699–715. [PubMed]

Sasaki, Y., Vanduffel, W., Knutsen, T., Tyler, C., & Tootell, R. (2005). Symmetry activates extrastriate visual cortex in human and nonhuman primates. *Proceedings of the National Academy of Sciences of the United States of America, 102,* 3159–3163. [PubMed] [Article]

Sclar, G., Maunsell, J. H., & Lennie, P. (1990). Coding of image contrast in central visual pathways of the macaque monkey. *Vision Research, 30,* 1–10. [PubMed]

Shams, L., & von der Malsburg, C. (2002). The role of complex cells in object recognition. *Vision Research, 42,* 2547–2554. [PubMed]

Shapley, R., Caelli, T., Grossberg, S., Morgan, M., & Rentschler, I. (1990). Computational theories of visual perception. *Visual perception: The neurophysiological foundations* (pp. 417–447). San Diego, CA: Academic Press.

Shapley, R., Hawken, M., & Ringach, D. L. (2003). Dynamics of orientation selectivity in the primary visual cortex and the importance of cortical inhibition. *Neuron, 38,* 689–699. [PubMed] [Article]

Somers, D. C., Nelson, S. B., & Sur, M. (1995). An emergent model of orientation selectivity in cat visual cortical simple cells. *Journal of Neuroscience, 15,* 5448–5465. [PubMed] [Article]

Spitzer, H., & Hochstein, S. (1985a). A complex-cell receptive-field model. *Journal of Neurophysiology, 53,* 1266–1286. [PubMed]

Spitzer, H., & Hochstein, S. (1985b). Simple- and complex-cell response dependences on stimulation parameters. *Journal of Neurophysiology, 53,* 1244–1265. [PubMed]

Szulborski, R. G., & Palmer, L. A. (1990). The two-dimensional spatial structure of nonlinear subunits in the receptive fields of complex cells. *Vision Research, 30,* 249–254. [PubMed]

Tadmor, Y., & Tolhurst, D. J. (1993). Both the phase and the amplitude spectrum may determine the appearance of natural images. *Vision Research, 33,* 141–145. [PubMed]

Tjan, B. S., Lestou, V., & Kourtzi, Z. (2006). Uncertainty and invariance in the human visual cortex. *Journal of Neurophysiology, 96,* 1556–1568. [PubMed] [Article]

Tootell, R. B., Hadjikhani, N., Hall, E. K., Marrett, S., Vanduffel, W., Vaughan, J. T., et al. (1998). The retinotopy of visual spatial attention. *Neuron, 21,* 1409–1422. [PubMed] [Article]

Touryan, J., Felsen, G., & Dan, Y. (2005). Spatial structure of complex cell receptive fields measured with natural images. *Neuron, 45,* 781–791. [PubMed] [Article]

Tsutsui, K., Sakata, H., Naganuma, T., & Taira, M. (2002). Neural correlates for perception of 3D surface orientation from texture gradient. *Science, 298,* 409–412. [PubMed]

van Hateren, J. H., & Ruderman, D. L. (1998). Independent component analysis of natural image sequences yields spatio-temporal filters similar to simple cells in primary visual cortex. *Proceedings of the Royal Society B: Biological Sciences, 265,* 2315–2320. [PubMed] [Article]

Wichmann, F. A., Braun, D. I., & Gegenfurtner, K. R. (2006). Phase noise and the classification of natural images. *Vision Research, 46,* 1520–1529. [PubMed]